Reactive uptake of HONO to TiO2 surface: "dark" reaction.

ARTICLE *in* THE JOURNAL OF PHYSICAL CHEMISTRY A · MARCH 2012

Impact Factor: 2.69 · DOI: 10.1021/jp300859w · Source: PubMed

2 AUTHORS:

Atallah El Zein
Université du Littoral Côte d'Opale (ULCO)
13 PUBLICATIONS **119** CITATIONS
SEE PROFILE

Yuri Bedjanian
CNRS Orleans Campus
67 PUBLICATIONS **861** CITATIONS
SEE PROFILE

THE JOURNAL OF PHYSICAL CHEMISTRY A

Article

pubs.acs.org/JPCA

Reactive Uptake of HONO to TiO_2 Surface: "Dark" Reaction

Atallah El Zein and Yuri Bedjanian*

Institut de Combustion, Aérothermique, Réactivité et Environnement (ICARE), CNRS, 45071 Orléans Cedex 2, France

ABSTRACT: The interaction of HONO with TiO_2 solid films was studied under dark conditions using a low pressure flow reactor (1−10 Torr) combined with a modulated molecular beam mass spectrometer for monitoring of the gaseous species involved. The reactive uptake of HONO to TiO_2 was studied as a function of HONO concentration ($[HONO]_0 = (0.3–3.3) \times 10^{12}$ molecules cm^{-3}), water concentration ($RH = 3 \times 10^{-4}$ to 13%), and temperature ($T = 275–320$ K). TiO_2 surface deactivation upon exposure to HONO was observed. The measured initial uptake coefficient of HONO on TiO_2 surface was independent of the HONO concentration and showed slight negative temperature dependence (activation factor = −1405 ± 110 K). In contrast, the relative humidity (RH) was found to have a strong impact on the uptake coefficient: $\gamma_0 = 1.8 \times 10^{-5} (RH)^{-0.63}$ (calculated using BET surface area, 40% uncertainty) at $T = 300$ K. NO_2 and NO were observed as products of the HONO reaction with TiO_2 surface with sum of their yields corresponding to nearly 100% of the nitrogen mass balance. The yields of the NO and NO_2 products were found to be 42 ± 7% and 60 ± 9%, respectively, independent of relative humidity, temperature, and concentration of HONO under experimental conditions used. The contribution of aerosol to the total HONO loss in the boundary layer (calculated with initial uptake data for HONO on TiO_2 surface) showed the unimportance of this process in the atmosphere. In addition, the diffusion coefficient of HONO in He was determined to be $D_{HONO-He} = 490 \pm 50$ Torr cm^2 s^{-1} at $T = 300$ K.

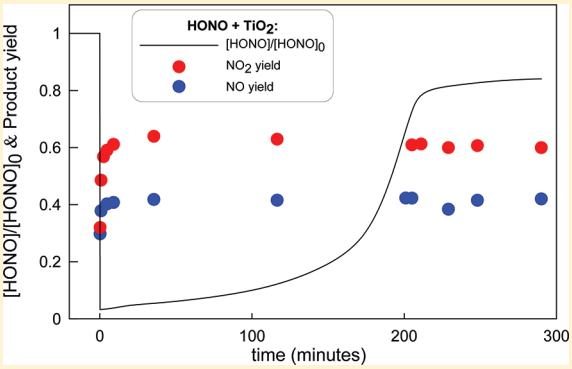

1. INTRODUCTION

HONO is an important atmospheric species representing a significant day time source (via photolysis) of OH radical, the major atmospheric oxidant. The mechanisms of HONO formation in the atmosphere are still not completely understood. One current issue in the chemistry of HONO is that the models fail to reproduce unexpectedly high daytime concentrations of HONO observed in the field studies, indicating the existence of new, yet unknown, daytime sources of HONO (e.g., ref 1) Heterogeneous processes, including those on humid surfaces, thought to be the major source of HONO in the atmosphere, were intensively studied in the laboratory and several mechanisms of HONO formation on aerosol and ground surface have been proposed.[1] However, in competition with heterogeneous HONO formation, the atmospheric aerosol can also act as a sink for gaseous HONO, probably, hardly competitive with HONO photolysis during the day, however potentially important at night-time. The information on the nature, rate and products of HONO interaction with solid surfaces of atmospheric interest is very scarce and seems to be limited to a few studies carried out with ice[2−5] and soot surface.[6,7] In addition, there have been several studies of the loss of HONO on "laboratory" surfaces such as Pyrex,[8,9] and borosilicate glass.[10]

The present paper is the first one in a series on systematic studies of the kinetics and products of the heterogeneous interaction of HONO with mineral aerosol and its different constituents and is focused on the reaction of HONO with TiO_2 surface. Titanium dioxide (TiO_2), although a minor component of mineral dust particles,[11] was shown recently to be responsible for the photochemical reactivity of atmospheric mineral aerosols.[12,13] Ndour et al.,[13] investigating the interaction of NO_2 with irradiated mixed TiO_2/SiO_2, Sahara dust and Arisona Test Dust films, have observed the formation of HONO for all samples, however, with varying yields. In this respect, it can be noted that kinetic and mechanistic information on HONO interaction with different surfaces seems to be very useful not only for atmospheric implications, but also for laboratory studies of the HONO forming heterogeneous processes where secondary surface reactions of HONO may have an impact on occurring chemistry and final HONO yield.

TiO_2 is a very efficient photocatalyst leading to the degradation of organic species under UV irradiation (e.g., ref 14) In addition, TiO_2 is known to transform nitrogen oxides (NO/NO_2), via catalytic heterogeneous reactions, to HNO_3, which remains on the TiO_2 surface.[15−19] Because of these photocatalytic properties, TiO_2 is widely used in a variety of so-called depolluting building materials aimed at removing the nitrogen oxides from the atmosphere. Recently, the antipolluting nature of the TiO_2-containing materials was questioned.[20−22] In particular, it was shown that the interaction of

Received: January 26, 2012
Revised: March 19, 2012
Published: March 19, 2012

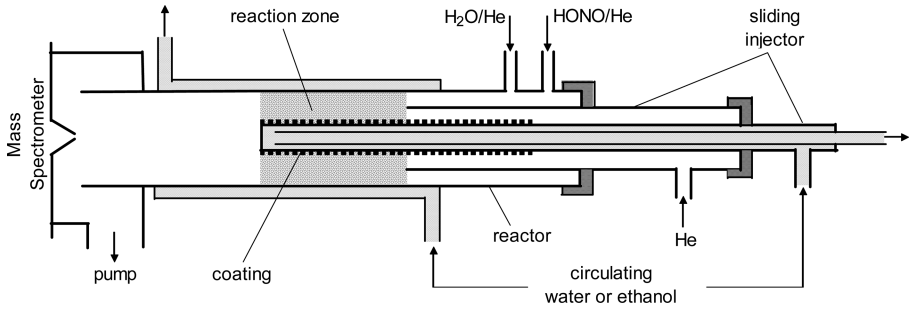

Figure 1. Diagram of the flow reactor used.

NO_2 with TiO_2[21] and commercial self-cleaning TiO_2-containig window glass[20] results in the formation of nitrous acid (HONO) in the gas phase. In contrast to mentioned studies, Laufs et al.[23] working with TiO_2 doped commercial paints observed an efficient decomposition of HONO on the photolytic samples and concluded that the paint surfaces do not represent a source of HONO.

On the basis of the above information, it is clear that experimental studies on the interaction of HONO with real mineral aerosols and their different constituents as well as with depolluting building materials containing TiO_2 are needed for better understanding of the heterogeneous sources and sinks of HONO in the atmosphere under dark and irradiation conditions. This paper reports the results of the experimental study of the kinetics and products of HONO interaction with TiO_2 surface under dark conditions. The detailed study of the reaction on the irradiated TiO_2 is a subject of our ongoing research.

2. EXPERIMENTAL SECTION

2.1. Preparation of TiO_2 Films. Solid TiO_2 films were deposited on the outer surface of a Pyrex tube (0.9 cm o.d.) using TiO_2 (Sigma Aldrich, Aeroxide P25, 50 ± 15 m^2 g^{-1} surface area, ~20 nm particle diameter) suspension in ethanol. Prior to film deposition, the Pyrex tube was treated with hydrofluoric acid and washed with distilled water and ethanol. Then the tube was immersed into the suspension, withdrawn and dried with a fan heater. As a result, rather homogeneous (to eye) films of TiO_2 were formed at the Pyrex surface. To eliminate the possible residual traces of ethanol, prior to uptake experiments, the freshly prepared TiO_2 samples were heated at 100−150 °C during 20−30 min under pumping.

2.2. Flow Reactor. Interaction of HONO with solid TiO_2 films was studied at 1−10 Torr total pressure (He being used as a carrier gas) using flow tube technique with mass spectrometric detection of the gaseous species involved. The experimental equipment and approach used for the kinetic measurements were described in previous papers from this group.[6,24] The main reactor (Figure 1) consisted of a Pyrex tube (40 cm length and 2.4 cm i.d.) with a jacket for the thermostatted liquid circulation. Experiments were carried out using a coaxial configuration of the flow reactor with movable central injector: the Pyrex tube with deposited sample was introduced into the main reactor along its axis. The coated tube could be moved relative to the outer tube of the injector that allowed the variation of the solid film length exposed to gas phase reactant and consequently of the reaction time.

2.3. Generation of HONO and Measurement of the Absolute Concentrations. HONO was generated via heterogeneous reaction of HCl with $NaNO_2$:

$$HCl + NaNO_2 \rightarrow HONO + NaCl$$

HCl diluted in He flowed through a column containing $NaNO_2$ crystals, and heterogeneously formed HONO was injected through the reactor side arm and detected at its parent peak as $HONO^+$ (m/z = 47). Under the experimental conditions used, this source of HONO was found to be free of residual concentration of HCl. Monitoring of the HCl concentration by mass spectrometry confirmed that HCl was completely consumed in reaction with $NaNO_2$ and did not reach the main reactor. This HONO source is known to be free of NO_2 and HNO_3.[25] In the present work, no signals were detected at m/z = 46 (NO_2^+), 63 (NO_3^+), and 64 (HNO_3^+) when HONO was present in the reactor. However, measurable concentration of NO coming from the HONO source was detected (10−20% of [HONO]) in agreement with the results of a previous study.[25]

Absolute concentrations of HONO were measured in situ using the method proposed previously.[25] This direct calibration method consisted of chemical conversion of HONO to NO_2 via the fast reaction with F atoms with subsequent detection and measurement of NO_2 concentration formed:

$$F + HONO \rightarrow HF + NO_2$$

H_2O was introduced into the reactor from a bubbler containing thermostatted (T = 298 K) deionized water. The concentrations of H_2O in the reactor were determined by calculating the H_2O flow rate from the total (H_2O + He) and H_2O vapor pressures in H_2O bubbler and the measured flow rate of He through the bubbler. The concentrations of the other stable species, in particular those of the reaction products NO and NO_2, were calculated from their flow rates obtained from the measurements of the pressure drop in calibrated volume flasks with the species diluted in helium. The estimated uncertainty on the measurements of the absolute concentrations of NO and NO_2 was less than 10%. All species were detected at their parent peaks. As NO^+ is a fragment of NO_2 and HONO, the NO signal at m/z = 30 was corrected for the fragmentation of NO_2 and HONO in the ion source of the mass spectrometer which operated at 25−30 eV.

3. RESULTS

3.1. Measurements of the Uptake Coefficient. Typical behavior of the HONO concentration upon introduction of the coated with TiO_2 tube into the reaction zone (in contact with HONO) is shown in Figure 2 (solid line). Fast initial consumption of HONO followed by progressive decrease of

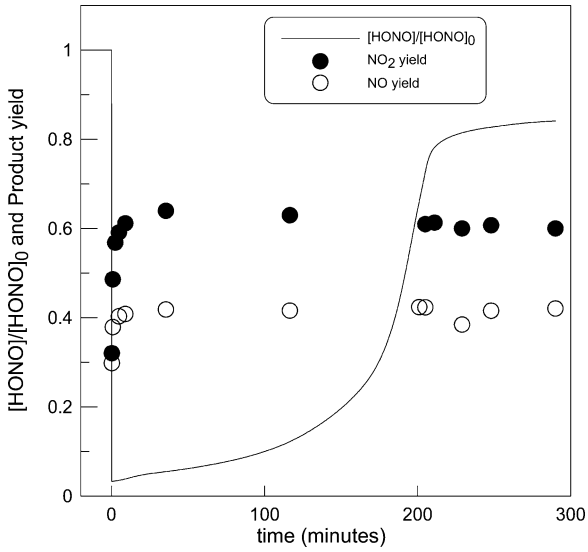

Figure 2. Normalized concentration of HONO (solid line) and the yield of the reaction products, NO and NO_2, as a function of exposure time of TiO_2 sample to HONO: T = 300 K, $[HONO]_0 = 2.0 \times 10^{12}$ molecules cm^{-3}, sample mass = 0.1 mg $cm^{-1} \times 14$ cm.

the HONO loss rate was observed. It was verified that when the TiO_2 sample was withdrawn from the reaction zone, that is, when HONO was no longer in contact with the TiO_2 surface, the HONO concentration rapidly recovered to its initial value. No additional HONO desorbed from the exposed TiO_2 surface was observed indicating the reactive character of the HONO + TiO_2 interaction which was also confirmed by the detection of the reaction products, NO and NO_2. In the example shown in Figure 2, one can note that stabilization of the HONO signal occurred after nearly 3.5 h of exposure. This quasi steady state HONO uptake, always at least an order of magnitude lower than the initial one, was found to decrease, although slowly, with exposure time. Consequently, in the present study, the measurements of the uptake coefficient were focused on its initial value corresponding to the first few minutes of the HONO exposure to TiO_2 film.

The uptake coefficient was determined as the probability of irreversible loss of the HONO molecules by collision with TiO_2 surface:

$$\gamma = \frac{4k'_{kin}}{\omega} \times \frac{V}{S} \qquad (I)$$

where k'_{kin} (in s^{-1}) is the first-order rate constant of the heterogeneous HONO loss in kinetic regime (see below), ω is the average molecular speed, V is the volume of the reaction zone and S is the surface area of the solid sample. The TiO_2 surface area (S) involved in the interaction with HONO was verified in specific experiments (see below). The rate constant of HONO loss was determined as

$$k'_{obs} = -\frac{d\ln([HONO])}{dt}$$

where k'_{obs} is the observed first-order rate constant of the heterogeneous loss of HONO and t is the reaction time defined by the ratio of the sample length to the flow velocity in the reactor. The initial rate of HONO loss was found to be independent of the HONO concentration: for $[HONO]_0$ varied in the range 2.7×10^{11} to 3.3×10^{12} molecules cm^{-3}, the measured values of k'_{obs} were similar within 10%. The measurements of the uptake coefficients described below were carried out with initial concentration of HONO of nearly 10^{12} molecules cm^{-3}.

3.1.1. Pressure Dependence. The measurements of the HONO loss rate (k'_{obs}) carried out at different pressures in the range 0.5−8.0 Torr have revealed their strong dependence on the total pressure in the reactor: the HONO loss rate was found to decrease as pressure increased. In fact, the loss rate of gas phase species on a surface is defined by two processes: transport of the species toward the surface and their heterogeneous reaction. When an efficient heterogeneous loss of the gaseous species leads to an important decrease of its concentration close to the reactive surface, the gas reactant diffusion from the volume toward the surface becomes rate limiting and should be taken into account for correct measurements of the uptake rate. For the determination of the first-order rate constant for the so-called kinetic regime, k'_{kin} (without of the diffusion limitation), the approach based on the kinetic resistance additivity rule is usually used:[26]

$$\frac{1}{k'_{obs}} = \frac{1}{k'_{kin}} + \frac{1}{k'_{dif}} \qquad (II)$$

where k'_{obs} is the first-order rate constant measured from the heterogeneous decay kinetics of gaseous reactant, k'_{kin} and k'_{dif} are the kinetic and diffusion limits of the rate constant, respectively. Present experiments were carried out using a coaxial configuration of the flow reactor with an active central rod (covered with TiO_2) and a passive surface of the main reactor (Pyrex) with respect to HONO. For this type of reactor configuration, k'_{dif} is defined by the following expression:[27,28]

$$k'_{dif} = K^d(q)\frac{D}{R^2}$$

where D is the diffusion coefficient of HONO in He, $K^d(q)$ is the dimensionless rate constant of radial diffusion, which is a function of the ratio $q = r/R$, r is the external radius of the coated tube and R is the internal radius of the main reactor. Thus, eq II can be written as:

$$\frac{1}{k'_{obs}} = \frac{1}{k'_{kin}} + \frac{R^2}{K^d(q)D_0} \times P \qquad (III)$$

where D_0 is the diffusion coefficient of HONO in He at 1 Torr pressure (Torr cm^2 s^{-1}) and P is the total pressure in the reactor (Torr of He).

The results of the measurements of k'_{obs} at different pressures are presented in Figure 3 as a dependence of reciprocal of k'_{obs} on total pressure of helium in the reactor. The pressure dependence experiments were carried out with the same partially deactivated TiO_2 sample under conditions of quasi steady state uptake in order to avoid significant decrease of k'_{obs} due to surface deactivation during the measurements at different pressures. Indeed, no significant decrease in surface reactivity occurred during the measurements, as shown by the results obtained at 1 Torr pressure at the beginning and the end of this series of experiments (Figure 3). The experimental data presented in Figure 3 can be well fitted with linear regression according to expression III: the intercept provides the value of $1/k'_{kin}$ and the slope of the straight line corresponds to $R^2/(K^d(q)D_0)$. These data in combination with $K^d(q) = 4.4$ (corresponding to the configuration of our system)[27] allow the

dx.doi.org/10.1021/jp300859w | J. Phys. Chem. A 2012, 116, 3665−3672

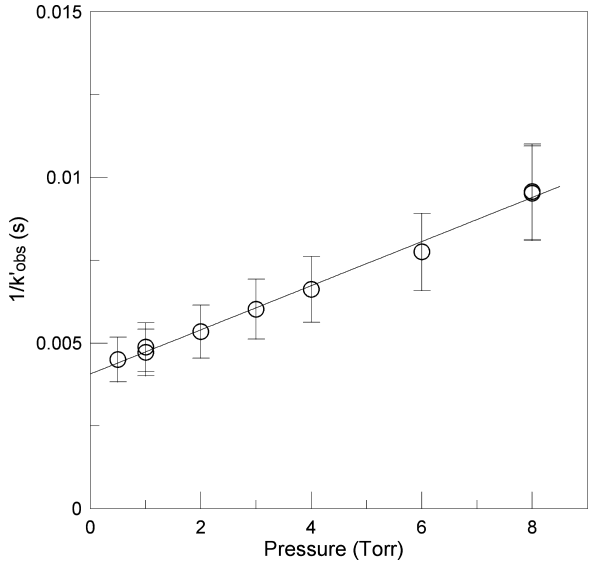

Figure 3. Reciprocal of the observed rate constant of HONO decay on TiO_2 surface as a function of the total pressure in reactor: T = 300 K, P = 0.5−8.0 Torr.

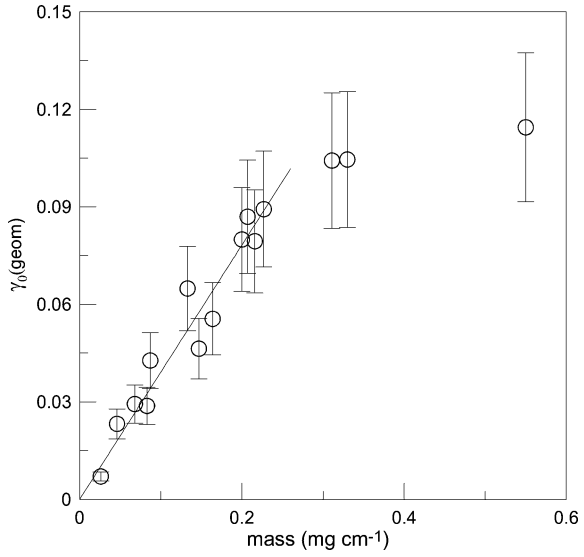

Figure 4. Dependence of the initial uptake coefficient of HONO (calculated using geometric surface area) on mass of TiO_2 sample (per 1 cm length of the support tube): T = 300 K, P = 1 Torr, sample mass = 0.03−0.55 mg cm^{-1}.

determination of D_0, the diffusion coefficient of HONO in He at 1 Torr total pressure and T = 300 K:

$$D_0 = 490 \pm 50 \text{ Torr cm}^2\text{s}^{-1}$$

where uncertainty is 2σ statistical one. Let us note that this value for the diffusion coefficient of HONO in He is in good agreement with those measured by Hirokawa et al.[29] (464 Torr cm^2 s^{-1} at T = 294 K) and estimated using the Fuller equation by Chu et al.[2] (515 Torr cm^2 s^{-1} at T = 300 K). The determined diffusion coefficient was used through this study (assuming $T^{1.75}$-dependence of D_0 on temperature) to determine k'_{kin} (via eq III) necessary for the calculations of the uptake coefficient (eq I). The experimental conditions for the measurements of the uptake coefficient were always chosen to minimize the diffusion corrections. The highest rates of HONO decay were measured at 1 Torr and the lowest rates (observed at highest RH) at nearly 10 Torr total pressure in the reactor. The diffusion corrections applied to k'_{obs} ranged from a few to 45% (for the highest k'_{obs}). Unless otherwise specified in the following text, for the purpose of simplicity, k' is used instead of k'_{kin}.

3.1.2. Dependence on Sample Mass. In these experiments, the HONO loss rate k'_0 was measured as a function of the thickness of TiO_2 coating with the purpose to determine the TiO_2 surface area involved in the interaction with HONO under experimental conditions used. The results of the measurements of the initial rate of the HONO uptake to TiO_2 under dry conditions (RH = 0.0003%) are shown in Figure 4 as a dependence of the uptake coefficient of HONO, γ_0(geom), calculated with geometric surface area on the mass of TiO_2 deposited per unity length of the support tube (which is equivalent to the thickness of the coating). One can note that two regimes were observed for γ_0(geom): the first one, where γ_0(geom) is linearly dependent on the mass of TiO_2 sample, and the second one (saturation region), where γ_0(geom) is independent of the sample mass. We consider that linear dependence of the reaction probability on mass, hence thickness, of TiO_2 film indicates that the entire surface area of the solid sample is accessible to HONO and, consequently, the BET surface area should be used for calculations of the true uptake coefficient. The uptake measurements in the present study were carried out with TiO_2 sample masses below 0.3 mg cm^{-1}, where linear dependence of the reaction rate on sample mass was observed and BET surface area of the TiO_2 samples was used to determine γ_0. The linear dependence in Figure 4 provides the following value of the initial uptake coefficient of HONO for RH used and T = 300 K:

$$\gamma_0 = (2.3 \pm 0.8) \times 10^{-3}$$

where uncertainty includes statistical one and those on BET surface area and on the measurements of k'_0. It should be noted that the value obtained for γ_0, calculated with BET surface area, should be considered as a lower limit of the uptake coefficient.

3.1.3. Dependence on Relative Humidity. In this series of experiments, the uptake of HONO was measured as a function of the partial pressure of water in the reactor. The pressure of water was varied between ~10^{-4} and 3 Torr, with the total pressure in the reactor in the range of 1−10 Torr. The results of these experiments are shown in Figure 5 as a dependence of γ_0 on relative humidity. A relatively strong negative dependence of the uptake coefficient on RH is observed. The solid line in Figure 5 represents a power fit to the experimental data and corresponds to the following expression:

$$\gamma_0 = 1.8 \times 10^{-5}(\text{RH})^{-0.63}$$

with estimated conservative 40% uncertainty on the uptake coefficient. The experiments were unfortunately limited to 12.6% RH in our low pressure flow reactor at room temperature.

3.1.4. Temperature Dependence. Temperature dependence of the uptake coefficient was measured in the temperature range 275−320 K. Relative humidity in these experiments was kept constant (RH = 0.001%) at all the temperatures. The uptake coefficient was found to slightly decrease with increasing temperature (Figure 6). The solid line in Figure 6 represents an

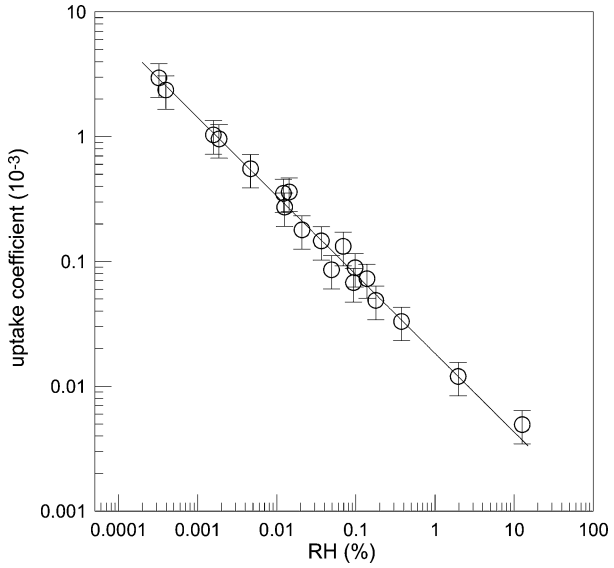

Figure 5. Uptake coefficient as a function of relative humidity: T = 300 K, P = 1−10 Torr.

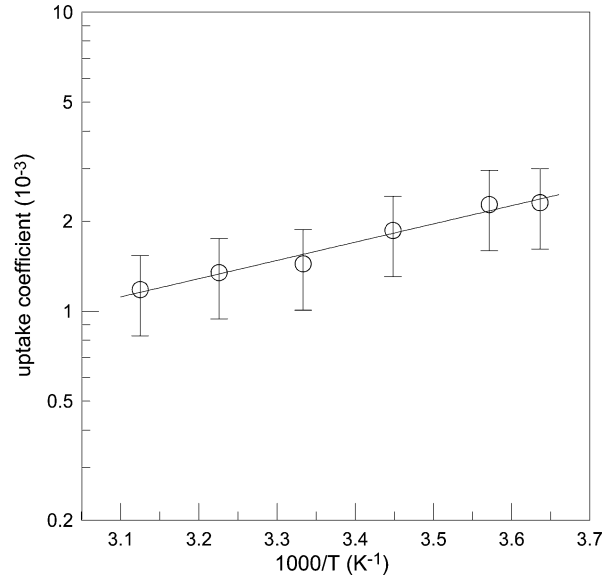

Figure 6. Temperature dependence of the uptake coefficient: P = 1 Torr, T = 275−320 K, RH = 0.001%.

exponential fit to the experimental data and provides the following Arrhenius expression for γ:

$$\gamma_0 = (1.4 \pm 0.5) \times 10^{-5} \exp[(1405 \pm 110)/T]$$

at T = 275−320 K (uncertainties are 1σ statistical ones).

3.2. Products Study. Experiments described in this section were focused on the determination of the products of the interaction of HONO with TiO_2 surface. Typical experiments consisted in the introduction of the TiO_2 sample into the reaction zone in contact with HONO and monitoring of the HONO concentration and those of the two gas phase products formed (NO and NO_2) under varied experimental conditions.

3.2.1. Dependence on Exposure Time. Figure 2 shows the yield of the reaction products (NO and NO_2) as a function of the exposure time of the TiO_2 film to HONO. The yield of the detected products was determined as a ratio of the product concentration formed to the concentration of HONO consumed:

$$\text{product yield} = \Delta[\text{product}]/\Delta[\text{HONO}]$$

One can note that time independent yields (except first phase of the exposure) of the detected products are observed during nearly 5 h of exposure and for the consumed fraction of HONO lying between 15 and 95%. The mean values of the products yields (61 and 41% for NO_2 and NO, respectively) lead to nearly 100% mass balance. The estimated uncertainties on the determination of the NO_2 and NO yields were nearly 15%. Possible reasons for the delayed formation of NO_2 observed during the first minutes of the reaction will be discussed later. It should be pointed out that all the measurements presented below were conducted under "stabilized" product yield conditions, that is, upon reaching the maximum NO_2 yield.

3.2.2. Dependence on Initial Concentration of HONO and Temperature. In this series of experiments, TiO_2 sample (mass = 11.2 cm × 0.25 mg cm^{-1}) was exposed to HONO concentration varied in the range (0.4−6.0) × 10^{12} molecules cm^{-3}. Figure 7 shows the concentrations of NO (open

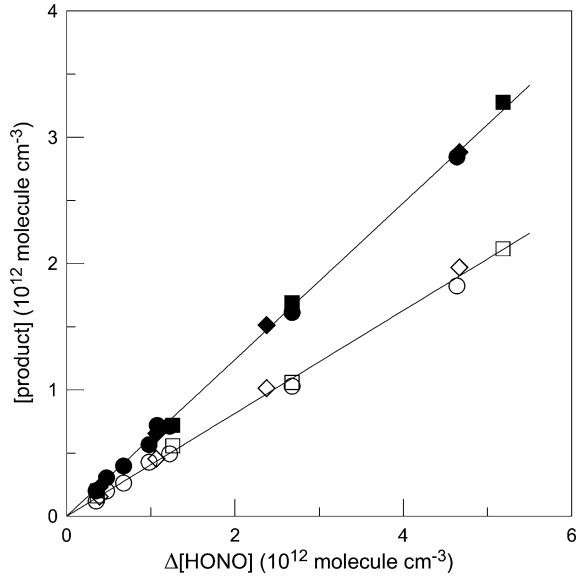

Figure 7. Dependence of the concentration of the products formed (open symbols, NO; filled symbols, NO_2) on the concentration of HONO consumed measured with initial concentration of HONO varied in the range (0.4−6.0) × 10^{12} molecules cm^{-3} and at three different temperatures in the reactor: diamonds, 275 K; circles, 300 K; squares, 320 K. Uncertainties on [NO] and [NO_2] are omitted for clarity.

symbols) and NO_2 (filled symbols) formed in the reaction of HONO with TiO_2 surface as a function of the consumed concentration of HONO. One can note that the impact of the initial concentration of HONO on the yield of the two detected products was negligible. Different symbols (diamonds, circles, and squares) in Figure 7 represent the data obtained at different temperatures in the reactor: 275, 300, and 320 K, respectively. As one can see, the impact of temperature on the distribution of the reaction products was also found to be negligible under the experimental conditions used. The straight lines in Figure 7 correspond to the linear through origin fits to the experimental

dx.doi.org/10.1021/jp300859w | J. Phys. Chem. A 2012, 116, 3665−3672

data and provide the branching ratios of 0.62 and 0.41 for NO_2 and NO forming pathways, respectively.

3.2.3. Dependence on Water Pressure. This series of experiments carried out at T = 300 K aimed at exploring the influence of water on the yield of the HONO + TiO_2 reaction products. The results of the measurements are shown in Figure 8 as a dependence of the NO_2 and NO yields on the concentration of H_2O present in the reactor. The maximum water concentration in these experiments was limited to nearly 10^{16} molecules cm^{-3}. The uptake of HONO is negatively dependent on water pressure, and at higher concentrations of H_2O, the consumed fraction of HONO and formed concentrations of NO and NO_2 were too low to be accurately measured. The variation of the concentration of water by 3 orders of magnitude was found to have no impact on the product yields of the heterogeneous reaction. The dashed lines in Figure 8 correspond to mean values of the measured NO_2 and NO yields: 0.59 and 0.43, respectively.

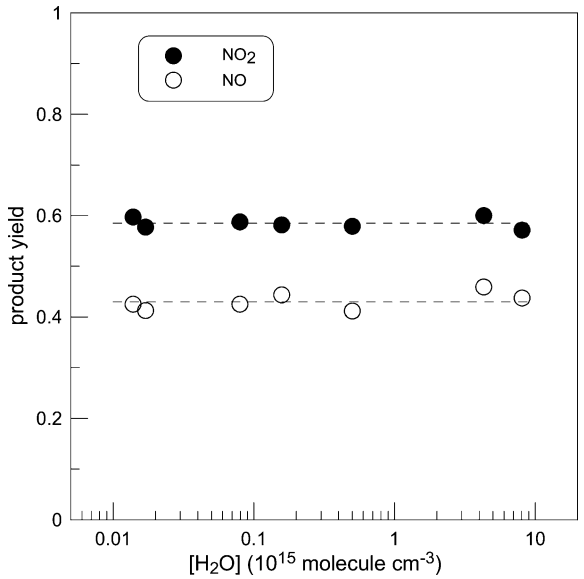

Figure 8. Branching ratio of the NO_2 and NO forming pathways (nearly 15% uncertainties are not shown) of the reaction of HONO with TiO_2 surface measured at different concentrations of water.

4. DISCUSSION

In the present study, two gas phase products, NO_2 and NO, were found to be formed in the heterogeneous reaction of HONO with TiO_2 surface with the yields of 60 ± 9 and 42 ± 6%, respectively. The branching ratios for the NO and NO_2 forming reaction pathways were shown to be independent of temperature (T = 275−320 K) and water pressure (3×10^{-4} to 0.3 Torr). Close results were reported by Syomin and Finlayson-Pitts[10] who observed equal yields for NO and NO_2 in their unconditioned glass cell under dry conditions. The formation of the equal amounts of NO and NO_2 was suggested to proceed via autoionization reaction between gas-phase and adsorbed HONO:

$$HONO_g + HONO_{ads} \rightarrow NO^+ + NO_2^- + H_2O$$

$$NO^+ + NO_2^- \rightarrow N_2O_3 \rightarrow NO + NO_2$$

Although the yields of NO_2 and NO measured in the present study for reaction of HONO with TiO_2 surface were not equal, the partial contribution of the above mechanism to the observed distribution of the reaction products cannot be excluded. On the other hand, additional (to those on glass surface) reaction pathways can be expected to occur on the more complex and more reactive TiO_2 surface. For instance, HONO can be oxidized by any Ti site which can be reduced (Ti^{4+}, Ti^{3+}):

$$HONO + \text{Ti site} \rightarrow NO_2 + H^+ + \text{reduced Ti site}$$

NO in turn could be formed via interaction of HONO with reduced Ti sites (Ti^{3+}, Ti^{2+}):

$$HONO + H^+ + \text{Ti site} \rightarrow NO + H_2O + \text{oxidized Ti site}$$

The possible secondary transformation of NO_2 formed on the surface can also influence the final distribution of the reaction products in the gas phase.

Syomin and Finlayson-Pitts[10] observed that with increasing RH the formation of NO was favored, and NO yield was greater than 90% at 50% RH. They reported that the mechanistic basis for the change in product yields as RH increases is not clear. Unfortunately, in the present study, this trend could not be verified for TiO_2 surface, as our data on products dependence on water is limited to much lower RH (∼1%).

As one can see in Figure 2, somewhat lower product yields (especially for NO_2) were measured in the first minutes of the TiO_2 exposure to HONO. The delayed NO_2 formation can be due to the secondary reaction of NO_2 with the TiO_2 surface with time-dependent rate (high initial uptake rapidly decreasing with exposure time). Similar effect of the delayed products formation was observed by Ten Brink and Spoelstra[9] in their study of the HONO loss on the wall of their Pyrex smog chamber. They reported that the first stage of the heterogeneous reaction was just removal of HONO from the gas phase, with only limited amounts of NO formed. On a longer time scale, the loss of HONO was compensated by the formation of NO and NO_2. As noted by the authors, this delayed formation of the products could be explained by their relatively slow desorption from the wall of the chamber, the preferential early release of NO reflecting the fact that this gas is less adsorptive than NO_2.

Negative dependence both on temperature and relative humidity was found for the initial uptake coefficient of HONO to TiO_2 surface in the present study. Similar effect of the decrease of the HONO loss rate with increasing RH was observed in previous studies carried out with glass surfaces.[8,10] Moreover, in the work of Kaiser and Wu,[8] the rate of HONO loss on the walls of a Pyrex reactor was found to decrease with increasing RH (from 0.2 to 5%) in accordance with an apparent reaction order in water concentration of −0.6, which is identical to that determined in the present study. The negative dependence of the HONO uptake rate on concentration of water was attributed to competition between HONO and H_2O for the available surface sites.[10]

Interestingly, the rather strong dependence of the uptake coefficient of HONO on relative humidity observed in the present study seems to correlate with relative humidity dependence of HONO chemistry derived from field measurements of HONO.[30] These authors reported that the [HONO]/[NO_2] ratios measured between 10 and 30% RH did not

exceed 0.04, while values of up to 0.09 were observed at higher RH. The results were analyzed using a simplified mechanism interpreting the observed maximum $[HONO]/[NO_2]$ ratio at a given relative humidity as the pseudo steady state (PSS) between the heterogeneous NO_2 to HONO conversion ($\gamma_{NO2\rightarrow HONO}$) and the HONO loss on surfaces (γ_{HONO}):

$$([HONO]/[NO_2])_{PSS} = \gamma_{NO_2\rightarrow HONO}/\gamma_{HONO}$$

With this approach, it is clear that RH dependence of the $([HONO]/[NO_2])_{PSS}$ is determined by the corresponding dependencies of the heterogeneous NO_2 to HONO conversion and HONO loss reactions. For example, the dependence on RH, $\gamma_{HONO} \sim (RH)^{-0.63}$, observed in the present study, leading to a decrease of γ_{HONO} by a factor of 2.4 between 20 and 80% RH, could account for the RH dependence of the HONO to NO_2 ratio, observed by Stutz et al.,[30] suggesting that HONO source is RH independent. Although this qualitative interpretation remains speculative (nature of aerosol, extrapolation of our data to higher RH, use of RH dependence for initial uptake which can be different for more atmospherically relevant steady state uptake), it seems to highlight the importance of the laboratory studies of HONO uptake on different surfaces of atmospheric relevance, including ground surface, and in extended range of RH.

The results on HONO uptake, although observed with pure TiO_2 samples, can be discussed in relation to atmospheric HONO chemistry occurring on aerosols and different types of ground surfaces. For instance, the potential loss of HONO on aerosol surface can be estimated using the present data and compared with HONO loss due to dry deposition which is main HONO sink process during night-time. The values reported for the deposition velocity of HONO range from 0.077 to 3 cm s^{-1} (Li et al.[31] and refs therein) which leads to the HONO deposition rate between 7.7×10^{-6} and 3×10^{-4} s^{-1} for 100 m height of the well mixed layer. In accordance with

$$k' = \frac{\omega\gamma}{4}\frac{S}{V}$$

and using $\gamma = 2 \times 10^{-6}$ measured in the present study (RH = 40%), aerosol surface loading of 10^{-6} to 10^{-5} cm^{-1},[32,33] typical for rural and urban atmosphere, the calculated value of HONO loss rate on aerosols is: $k' \sim 1.5 \times 10^{-8}$ to 1.5×10^{-7} s^{-1} (for RH = 40%, T = 300 K). This value is, at least, by a factor of 50 lower than the dry deposition rate of HONO. Thus, the contribution of aerosol to the total HONO loss in the boundary layer (calculated with uptake data for TiO_2 surface) seems to be very limited. It should be noted that in the calculations above, the initial (i.e., highest) uptake coefficient of HONO was used: it means that in the atmosphere, where airborne dust particles have an average lifetime of a couple of days and are at least partly passivated (deactivated), the HONO heterogeneous loss is expected to be even less important. However, the correct assessment of the HONO loss rate on the atmospheric aerosols requires additional experimental data on HONO uptake on different surfaces representative of the atmospheric particulate material.

To our knowledge, this is the first direct study of the heterogeneous HONO interaction with mineral oxide surface. Laufs et al.[23] studying NO_2 interaction with TiO_2 doped commercial paints observed nitrous acid formation in the dark and its efficient decomposition under UV irradiation. For the photolytic uptake coefficient of HONO, the value of $\gamma = (2–9) \times 10^{-5}$ was determined (for RH in the range 10−85%). These values are higher than those expected from the present study for this RH-range under dark conditions. In addition, in contrast to the present data for dark uptake, the photocatalytic decomposition of HONO was found to increase with increasing humidity. The decomposition of HONO on the photolytic samples was attributed to hydrolysis of HONO following by further oxidation of NO_2^- formed:

$$HONO + H_2O \leftrightarrow NO_2^- + H_3O^+$$

It seems that this mechanism is not operative under dark conditions of the present study, where strong decrease of the HONO uptake rate with increasing concentration of water was observed. It should be noted that for a photocatalyst such as TiO_2 the difference of the kinetics for a dark reaction compared to that for a photocatalytic reaction could be expected since additional reaction mechanisms are switched on in the presence of light. Another point to emphasize in relation to above comparison is that the surface properties of the paint samples (alkaline) used by Laufs et al.[23] and P25 TiO_2 (acidic) used in the present study are different. In relation to the depolluting nature of the TiO_2 doped materials, present results on the reaction products show that even if HONO is taken up by these materials it is stoichiometrically converted to NO_x (at least, during night-time). To fully clarify the question, direct measurements of the rate and products of HONO interaction with TiO_2 under irradiation would be very useful.

AUTHOR INFORMATION

Corresponding Author

*Tel.: +33 238255474. Fax: +33 238696004. E-mail: yuri.bedjanian@cnrs-orleans.fr.

Notes

The authors declare no competing financial interest.

ACKNOWLEDGMENTS

This study was supported by LEFE − CHAT programme of CNRS (Photona project) and ANR from Photodust grant. A.E.Z. is very grateful to région Centre for financing his Ph.D. grant. The authors are very grateful to both reviewers for their helpful comments and especially to one of them for the comment on the possible reaction mechanism.

REFERENCES

(1) Kleffmann, J. *ChemPhysChem* **2007**, *8*, 1137.
(2) Chu, L.; Diao, G.; Chu, L. T. *J. Phys. Chem. A* **2000**, *104*, 3150.
(3) Diao, G.; Chu, L. T. *J. Phys. Chem. A* **2005**, *109*, 1364.
(4) Fenter, F. F.; Rossi, M. J. *J. Phys. Chem.* **1996**, *100*, 13765.
(5) Kerbrat, M.; Huthwelker, T.; Bartels-Rausch, T.; Gaggeler, H. W.; Ammann, M. *Phys. Chem. Chem. Phys.* **2010**, *12*, 7194.
(6) Lelièvre, S.; Bedjanian, Y.; Laverdet, G.; Le Bras, G. *J. Phys. Chem. A* **2004**, *108*, 10807.
(7) Stadler, D.; Rossi, M. J. *Phys. Chem. Chem. Phys.* **2000**, *2*, 5420.
(8) Kaiser, E. W.; Wu, C. H. *J. Phys. Chem.* **1977**, *81*, 1701.
(9) Ten Brink, H. M.; Spoelstra, H. *Atmos. Environ.* **1998**, *32*, 247.
(10) Syomin, D. A.; Finlayson-Pitts, B. J. *Phys. Chem. Chem. Phys.* **2003**, *5*, 5236.
(11) Karagulian, F.; Santschi, C.; Rossi, M. J. *Atmos. Chem. Phys.* **2006**, *6*, 1373.
(12) Gustafsson, R. J.; Orlov, A.; Griffiths, P. T.; Cox, R. A.; Lambert, R. M. *Chem. Commun.* **2006**, 3936.
(13) Ndour, M.; D'Anna, B.; George, C.; Ka, O.; Balkanski, Y.; Kleffmann, J.; Stemmler, K.; Ammann, M. *Geophys. Res. Lett.* **2008**, *35*, L05812.

(14) Henderson, M. A. *Surf. Sci. Rep.* **2011**, *66*, 185.
(15) Dalton, J. S.; Janes, P. A.; Jones, N. G.; Nicholson, J. A.; Hallam, K. R.; Allen, G. C. *Environ. Pollut.* **2002**, *120*, 415.
(16) Devahasdin, S.; Fan, C. Jr.; Li, K.; Chen, D. H. *J. Photochem. Photobiol., A* **2003**, *156*, 161.
(17) Ibusuki, T.; Takeuchi, K. *J. Mol. Catal.* **1994**, *88*, 93.
(18) Negishi, N.; Takeuchi, K.; Ibusuki, T. *J. Mater. Sci.* **1998**, *33*, 5789.
(19) Ohko, Y.; Nakamura, Y.; Fukuda, A.; Matsuzawa, S.; Takeuchi, K. *J. Phys. Chem. C* **2008**, *112*, 10502.
(20) Langridge, J. M.; Gustafsson, R. J.; Griffiths, P. T.; Cox, R. A.; Lambert, R. M.; Jones, R. L. *Atmos. Environ.* **2009**, *43*, 5128.
(21) Monge, M. E.; D'Anna, B.; George, C. *Phys. Chem. Chem. Phys.* **2010**, *12*, 8991.
(22) Ndour, M.; Conchon, P.; D'Anna, B.; Ka, O.; George, C. *Geophys. Res. Lett.* **2009**, *36*, L05816.
(23) Laufs, S.; Burgeth, G.; Duttlinger, W.; Kurtenbach, R.; Maban, M.; Thomas, C.; Wiesen, P.; Kleffmann, J. *Atmos. Environ.* **2010**, *44*, 2341.
(24) Loukhovitskaya, E.; Bedjanian, Y.; Morozov, I.; Le Bras, G. *Phys. Chem. Chem. Phys.* **2009**, *11*, 7896.
(25) Bedjanian, Y.; Lelièvre, S.; Bras, G. L. *J. Photochem. Photobiol., A* **2004**, *168*, 103.
(26) Frank-Kamenetskii, D. A. *Diffusion and Heat Transfer in Chemical Kinetics*; Plenum Press: New York, London, 1969.
(27) Gershenzon, Y. M.; Grigorieva, V. M.; Ivanov, A. V.; Remorov, R. G. *Faraday Discuss.* **1995**, *100*, 83.
(28) Gershenzon, Y. M.; Grigorieva, V. M.; Zasypkin, A. Y.; Remorov, R. G. Theory of radial diffusion and first order wall reaction in movable and immovable media; *Proceedings of the 13th International Symposium on Gas Kinetics*, Dublin, Ireland, 1994.
(29) Hirokawa, J.; Kato, T.; Mafuné, F. *J. Phys. Chem. A* **2008**, *112*, 12143.
(30) Stutz, J.; Alicke, B.; Ackermann, R.; Geyer, A.; Wang, S.; White, A. B.; Williams, E. J.; Spicer, C. W.; Fast, J. D. *J. Geophys. Res.* **2004**, *109*, D03307.
(31) Li, X.; Brauers, T.; Häseler, R.; Bohn, B.; Hofzumahaus, A.; Holland, F.; Lu, K. D.; Rohrer, F.; Hu, M.; Zeng, L. M.; Zhang, Y. H.; Garland, R.; Su, H.; Nowak, A.; Takegawa, N.; Shao, M.; Wahner, A. *Atmos. Chem. Phys. Discuss.* **2011**, *11*, 27591.
(32) Seinfeld, J. H.; Pandis, S. N. *Atmospheric Chemistry and Physics*; Wiley-Interscience: New York, 1998.
(33) Wehner, B.; Wiedensohler, A. *Atmos. Chem. Phys.* **2003**, *3*, 867.